Fluorescence and absorption assessment of a lipid mTHPC formulation following topical application in a non-melanotic skin tumor model.

Johansson, Ann; Svensson, Jenny; Bendsöe, Niels; Svanberg, Katarina; Alexandratou, Eleni; Kyriazi, Maria; Yova, Dido; Grafe, Susanna; Trebst, Tilmann; Andersson-Engels, Stefan

Published in:
Journal of Biomedical Optics

DOI:
10.1117/1.2743080

2007

Fluorescence and absorption assessment of a lipid mTHPC formulation following topical application in a non-melanotic skin tumor model

Ann Johansson
Jenny Svensson
Lund University
Department of Physics
P.O. Box 118
SE-221 00 Lund, Sweden

Niels Bendsoe
Lund University Hospital
Department of Dermatology and Venereology
SE-221 85 Lund, Sweden

Katarina Svanberg
Lund University Hospital
Department of Oncology
SE-221 85 Lund, Sweden

Eleni Alexandratou
Maria Kyriazi
Dido Yova
National Technical University of Athens
Department of Electrical Engineering and Computing
Biomedical Optics and Applied Biophysics Laboratory
G-15780 Athens, Greece

Susanna Gräfe
Biolitec AG
Research and Development
D-07745 Jena, Germany

Tilmann Trebst
CeramOptec GmbH
D-53121 Bonn, Germany

Stefan Andersson-Engels
Lund University
Department of Physics
P.O. Box 118
SE-221 00 Lund, Sweden

Abstract. Although the benefits of topical sensitizer administration have been confirmed for photodynamic therapy (PDT), ALA-induced protoporphyrin IX is the only sensitizer clinically used with this administration route. Unfortunately, ALA-PDT results in poor treatment response for thicker lesions. Here, selectivity and depth distribution of the highly potent sensitizer *meso*-tetra(hydroxyphenyl)chlorin (mTHPC), supplied in a novel liposome formulation was investigated following topical administration for 4 and 6 h in a murine skin tumor model. Extraction data indicated an average [± standard deviation (SD)] mTHPC concentration within lesions of 6.0(±3.1) ng/mg tissue with no significant difference ($p<0.05$) between 4- and 6-h application times and undetectable levels of generalized photosensitivity. Absorption spectroscopy and chemical extraction both indicated a significant selectivity between lesion and normal surrounding skin at 4 and 6 h, whereas the more sensitive fluorescence imaging setup revealed significant selectivity only for the 4-h application time. Absorption data showed a significant correlation with extraction, whereas the results from the fluorescence imaging setup did not correlate with the other methods. Our results indicate that this sensitizer formulation and administration path could be interesting for topical mTHPC-PDT, decreasing the effects of extended skin photosensitivity associated with systemic mTHPC administration. [DOI: 10.1117/1.2743080]

Keywords: pharmacokinetics; fluorescence imaging; absorption spectroscopy; photodynamic therapy; mTHPC.

Paper 06158RR received Jun. 12, 2006; revised manuscript received Feb. 19, 2007; accepted for publication Feb. 20, 2007; published online May 22, 2007. This paper is a revision of a paper presented at the SPIE conference on Optical Diagnostics and Sensing VI, Jan. 2006, San Jose, Calif. The paper presented there appears (unrefereed) in SPIE Proceedings Vol. 6094.

1 Introduction

Photodynamic therapy (PDT) as a cancer treatment modality has shown promising results both in terms of efficacy and selectivity.[1] The PDT effect is caused by a combination of treatment induced apoptosis and direct necrosis,[2] vascular damage,[3] and possibly an elicited immune response,[4] where the extent of tissue damage depends on the total light dose, the tissue oxygenation, and the sensitizer concentration.[5] The most common administration route is intravenous injection, leading to an extended photosensitivity following treatment for some sensitizers.[6]

In the case of easily accessible and thin lesions, e.g., superficial skin malignancies, topical sensitizer application is highly desirable from a clinical point of view. ALA-induced protoporphyrin IX is a photosensitizer that has been used with this administration route for the treatment of various skin

Address all correspondence to Ann Johansson, Department of Physics, Lund University, PO Box 118-Lund, 221 00 Sweden; Tel: +46462223120; Fax: +46462224250; E-mail: ann.johansson@fysik.lth.se

1083-3668/2007/12(3)/034026/9/$25.00 © 2007 SPIE

tumors.[7] To overcome the poor skin permeability caused by the hydrophilic character of the ALA molecule, several groups have investigated the selectivity and penetration depths of some of its esters. Utilizing the less hydrophilic methyl esterified ALA-Me, good tumor selectivity has been observed both in animal skin tumor models and in human basal cell carcinomas[8,9] (BCCs). However, the limited light penetration of the activating light,[10] the localization of the protoporphyrin IX molecule within biological tissue,[11] and the relatively low extinction coefficient of this sensitizer[12] are additional factors that might limit the treatment efficacy.[7,13]

In contrast to protoporphyrin IX, *meso*-tetra(hydroxyphenyl)chlorin (mTHPC) has been reported as one of the most efficient sensitizers, as relatively small drug and light doses are required to achieve treatment response.[14] However, the hydrophobic mTHPC molecules form aggregates in aqueous surroundings, leading to limited transportation of the sensitizer within biological media, tumor selectivity, and PDT efficacy.[15–17] Gupta et al.[18] reported on PDT following topical mTHPC administration for treatment of Bowen's disease and BCCs. In this study, the overall pathological tumor clearance was limited to 32% at the 2-month follow-up. The authors suggest the method of topical sensitizer application and mTHPC formulation were the primary limiting factors. In an effort to improve efficiency of topically administered drugs, the use of liposomes as drug delivery vehicles has been reported to increase skin penetration for some active substances.[19] For example, ALA has been encapsulated into liposomes, leading to an improved retention within the epidermis and dermis in an *in vitro* skin model.[20] By incorporating the hydrophobic PDT agent bacteriochlorin into liposomes, an increased oxygen consumption and decreased cell survival during PDT in cell cultures was observed as compared to the raw formulation.[21] Furthermore, the use of liposomes as carrier of benzoporphyrin derivative monoacid ring A resulted in better PDT efficiency in a mouse tumor model.[22] These effects have been explained by monomerization of the sensitizer,[21] a different microlocalization within the cells and an increased association with low density lipoproteins when incorporating the sensitizers into liposomes.[21,22]

In this paper, the sensitizer distribution following topical application of a novel gel formulation containing liposome-encapsulated mTHPC, referred to as mTHPC-gel, is investigated in an animal skin tumor model. The drug-accumulation interval in this study is restricted to 4 and 6 h, as clinically relevant for topically applied PDT photosensitizers.[23] In addition, the application of this new mTHPC formulation for several hours is possible as the compound is supplied in a heat-setting gel. Chemical extraction and noninvasive optical methods are utilized for investigating the selectivity between lesion and normal skin. In addition, the mTHPC concentration within the internal organs is monitored to assess the level of generalized photosensitivity.

A further incentive of the present study is the comparison of fluorescence and absorption spectroscopy to chemical extraction as methods for quantifying sensitizer concentration. The combination of a strongly fluorescing and absorbing PDT agent and superficially located lesions makes fluorescence imaging and absorption spectroscopy attractive tools for noninvasive studies of sensitizer concentration. These methods have the additional advantage that they can provide information in real time. On the other hand, as the fluorescence signal depends on tissue optical properties, it is difficult to utilize the absolute fluorescence level to quantify the sensitizer concentration, especially within heterogeneous media. For the absorption spectroscopy data, the effect of varying tissue absorption can be handled by studying the total absorption imprint of tissue and exogenous chromophore over a sufficiently broad spectral interval.

In this work, imaging of the tissue and sensitizer fluorescence levels is performed utilizing a near-UV light source and detection at a few selected wavelengths. The absorption spectroscopy setup utilizes a fiber optical source-detector pair, where the source-detector separation has been chosen to make the method insensitive to variations in scattering parameters for the range of scattering values typically found in biological tissue.[24] The predicted sensitizer concentration is tested for correlation between the two optical methods and the chemical extraction and we comment on the accuracy of the optical methods for this tumor model and measurement geometry.

2 Materials and Methods

2.1 *mTHPC-gel Preparation*

The compound is comprised of a liposomal formulation of mTHPC in a thermogel matrix (biolitec AG, Jena, Germany) with a sensitizer concentration of 0.5 mg mTHPC/ml gel. The liposome formulation (Foslip) is based on dipalmitoylphosphatidylcholine (DPPC), monosaccharide, water, and polyoxyethylene polyoxypropylene block copolymers and encapsulates the mTHPC (Ref. 25). The mTHPC-gel is liquid at the storage temperature of 4 °C but forms a highly viscous gel when heated by the skin to temperatures above 26 °C. The thermothickening thus aids in increasing the retention time of the applied gel and transfer of the sensitizer into the tissue. No penetration enhancers are added to the mTHPC-gel.

2.2 *Animal Procedures*

Malignant skin tumors were induced in seven male albino hairless mice (SKH-HR1), 8 to 10 weeks old and weighing 30 to 35 g. For skin carcinoma induction, a two-stage model of carcinogenesis was utilized with DMBA [7,12-dimethylbenz(a)anthracene] as initiator and ultraviolet radiation as skin cancer promoter. Details on the procedure for induction of skin carcinogenesis have been published by Kyriazi et al.[26] Tumors first appear as benign papillomas, progressing toward more malignant states, and finally developing into basal (10%) and squamous (80%) cell carcinomas as determined after histopathological examination of representative specimens. In the remaining 10%, no malignant transformation appears. This progress is consistent with previously described studies in hairless mice.[27] Here, tumor diameters ranged between 0.2 and 1 cm, where mice with tumor diameter greater than 1 cm were euthanatized for ethical reasons. The study was carried out according to the guidelines established by the European Parliament and Council Directive 2003/65/EC and the Greek Animal Ethics Committee.

Twenty microliters of mTHPC-gel was applied topically on each of the areas investigated, i.e., tumor, normal skin, and skin in the immediate vicinity of the tumor. The sensitizer concentration was studied at 4 or 6 h after mTHPC-gel administration utilizing noninvasive optical techniques. Three

animals with a total of 10 lesions and another three animals with 5 lesions were investigated at the 4- and 6-h time points, respectively. All tissue regions were carefully cleaned prior to fluorescence and absorption measurements to remove any gel remaining on the skin surface. In addition, the optical measurements were performed on all animals prior to administration of the mTHPC-gel. For all animals, application of the sensitizer and optical measurements were performed under general anesthesia [intraperiteneal (i.p.) injection of 20 μl of γ-hydroxybutiric lactone solution in 0.9% sodium chloride (50:50, v:v)]. Following the optical measurements at 4 or 6 h, animals were killed by cervical dislocation and the tissue regions previously treated with the mTHPC-gel were excised for extraction measurements. In addition, the mTHPC concentration in blood, liver, spleen, muscle, and normal skin where no sensitizer had been applied was also investigated by means of extraction.

In vivo optical measurements were also performed for two lesions in another animal at 1.5, 3, and 5 h after sensitizer application in an attempt to follow the temporal mTHPC concentration profile within a single animal. However, prior to the spectroscopic investigations at 1.5, 3, and 5 h, the tissue regions had to be carefully cleaned to avoid measuring fluorescence from mTHPC within the gel remaining only on top of the skin surface. After the optical measurements at 1.5 and 3 h, another 20 μl of the mTHPC-gel was administered to enable further sensitizer accumulation. This procedure was thus slightly different from that employed for the remaining animals as it resulted in the application of three 20-μl aliquots of the sensitizer gel. After sacrificing the animal at the 5-h drug-light interval, the mTHPC fluorescence and absorption levels were also investigated throughout a vertical cut of the two excised tumors to study the depth distribution.

2.3 *Fluorescence Imaging*

A 405-nm continuous-wave diode laser (Power Technology Inc., Little Rock, Arkansas) emitting 2.1 mW was used to induce fluorescence within a 27-mm-diam area. The tissue autofluorescence at 500 (±10 nm) and mTHPC fluorescence at 654 nm (±20 nm) were filtered out using bandpass filters (Oriel, Stratford, Connecticut) and imaged using a cooled, intensified CCD (iStar, Andor Technology, Belfast, Northern Ireland). Two cut-off filters, GG475 and GG455 (Schott, Mainz, Germany), were used to attenuate the reflected excitation light. All data was compensated for differences in spectral response using a National Institute of Standards and Technology (NIST)-traceable light source.

For each animal, the fluorescence intensities at 654 and 500 nm were averaged within each investigated tissue region. The mTHPC distribution was quantified by a dimensionless contrast function resulting from forming a spectral ratio between the two detection bands:

$$F = \frac{I(654\ \text{nm}) - I_{\text{bkg}}}{I(500\ \text{nm}) - I_{\text{bkg}}}, \tag{1}$$

where $I(654\ \text{nm})$ and $I(500\ \text{nm})$ denote the fluorescence intensity at the two wavelengths, and I_{bkg} is a constant background level originating from the dark current of the detector.

For this setup, the mTHPC detection limit was below 0.005 μM in liquid phantoms containing ink (Pelikan Fount India Ink, Hannover, Germany) at volume concentrations of 0.35 to 1.05%, giving background absorption of 0.2 to 0.6 cm^{-1}, and Intralipid (Fresenius Kabi, Uppsala, Sweden) at volume concentrations of 2.8 to 3.7%, resulting in a reduced scattering coefficient between 7 and 9 cm^{-1}.

2.4 *Absorption Spectroscopy*

The optical absorption setup together with the accuracy and validity of the method have been described in greater detail elsewhere.[24,28] Briefly, the output from a pulsed xenon short-arc lamp was delivered by a 400-μm-diam optical fiber and, after interacting with the tissue, the transmitted light was collected by a 200-μm-diam fiber. The center-to-center distance between delivery and collection fibers measured 2.0 mm. An S2000 miniature spectrometer (Ocean Optics Inc., Dunedin, Florida) was used to disperse and detect the collected light. Wavelength-dependent fluctuations in source output and detector response were accounted for by taking a reference measurement from a spectrally flat diffuse reflector based on Spectralon material (Lab Sphere Inc., Cranfield, UK) in connection to each measurement sequence.

For source-detector separations in the range 1.5 to 2.6 mm, the path length of the collected photons has been shown to be relatively insensitive to variations in tissue scattering.[24] Therefore, Beer-Lambert's law can be used to assess changes in tissue absorption. The negative logarithm of the transmission signal measured after the addition of an absorber, $I_2(\lambda) = I(\Delta\mu_a + \mu_a^0)$, to that before, $I_1(\lambda) = I(\mu_a^0)$, is given by[28]

$$R(\lambda) = -\ln\left(\frac{I_2}{I_1}\right) = -\ln\left[\frac{I(\Delta\mu_a + \mu_a^0)}{I(\mu_a^0)}\right] = \Delta\mu_a L_{\text{eff}}(\Delta\mu_a + \mu_a^0) + B. \tag{2}$$

In Eqs. (2) to (6), the wavelength dependence of the absorption coefficients and the transmission signals is omitted for the purpose of clarity. Although the path length is insensitive to scattering variations, the amount of collected light might change between measurements and hence the appearance of the factor B. Here, $L_{\text{eff}}(\Delta\mu_a + \mu_a^0)$ denotes the effective path length, which depends on the total absorption coefficient. To determine this dependence, a nonsequential ray tracing software package (ASAP 8.0.3, Breault Research Organization, Tucson, Arizona) was used to track the pathlengths of collected rays for a geometry matching the experimental setup. For these simulations, the source and detection fibers, having diameters as already stated and a numerical aperture of 0.22, were separated by 2 mm. The scattering and anisotropy coefficients were kept constant at 10 cm^{-1} and 0.9, respectively. We simulated 167 million rays in the absence of absorption and the optical path lengths L_i for all detected rays were stored. The effect of tissue absorption on the optical path lengths was added to the simulation results and the effective path length for different absorption coefficients was evaluated by

$$L_{\mathrm{eff}}(\mu_a) = -\frac{1}{\mu_a}\ln\left[\frac{\sum_{i=1}^{N}\exp(-\mu_a L_i/n)}{N}\right]. \quad (3)$$

Here n denotes the refractive index, and N equals the number of detected rays, in this case 1.4 and 1000, respectively. The absorption coefficient μ_a was allowed to vary between 0.001 and 5 cm^{-1} in steps of 0.001 cm^{-1}. In contrast to the work by Mourant et al.,[28] where a slightly smaller fiber separation was used, no single functional dependency could adequately fit the effective path length to the total absorption coefficient over the entire absorption range. Therefore, a nearest-neighbor spline interpolation was used to describe the dependence of the effective path length on the total absorption coefficient.

In earlier work, Eq. (2) was in fact evaluated from measurements before and after addition of an exogenous absorber.[28] Here, both I_1 and I_2 are evaluated from a single measurement. By assuming that tissue absorption at 900 nm is dominated by water at a constant concentration of 60%, I_1 can be expressed as

$$\begin{aligned} I_1 = I(\mu_a^{60\%\ \mathrm{water}}) = I(900\ \mathrm{nm}) \\ \times\exp[-L_{\mathrm{eff}}(\mu_a^{60\%\ \mathrm{water}})\mu_a^{60\%\ \mathrm{water}}]\cdots \\ \times\exp\{-L_{\mathrm{eff}}[\mu_a^{60\%\ \mathrm{water}}(900\ \mathrm{nm})] \\ \times\mu_a^{60\%\ \mathrm{water}}(900\ \mathrm{nm})\}^{-1}, \end{aligned} \quad (4a)$$

where $I(900\ \mathrm{nm})$ is the detected signal at 900 nm. Furthermore, I_2 is given by the detected signal and is described, as before,

$$I_2 = I(\Delta\mu_a + \mu_a^0) = I(\Delta\mu_a + \mu_a^{60\%\ \mathrm{water}}). \quad (4b)$$

Since both transmission signals originate from a single measurement, the factor B is eliminated and Eq. (2) is modified to

$$\begin{aligned} R(\lambda) &= -\ln\left[\frac{I(\Delta\mu_a + \mu_a^{60\%\ \mathrm{water}})}{I(\mu_a^{60\%\ \mathrm{water}})}\right] \\ &= \Delta\mu_a L_{\mathrm{eff}}(\Delta\mu_a + \mu_a^{60\%\ \mathrm{water}}). \end{aligned} \quad (5)$$

The function "lsqnonlin" in MATLAB (MathWorks, Natick, Massachusetts) was used to solve for $\Delta\mu_a$ from Eq. (5). The spectral fitting interval was 500 to 800 nm. A singular value decomposition (SVD) algorithm was used to fit the extinction coefficients of relevant tissue chromophores to the calculated change in absorption coefficient. The SVD algorithm provides the best fit of a linear combination of a certain number of basis spectra to a data set and has been used previously in order to analyze fluorescence[29] and broad-banded reflectance spectra.[30] The extinction coefficients included in the evaluation of the absorbance data were those of mTHPC, deoxy- (Hb) and oxyhemoglobin[31](HbO). In addition, the mTHPC fluorescence spectrum was included in the model since experimental work gave evidence that the shorter wavelengths within the light source did induce detectable sensitizer fluorescence also in the presence of strong tissue absorption. This fluorescence component partly overlaps the absorption peak at 652 nm, leading to an underestimated mTHPC concentration if fitting the sensitizer extinction coefficient to this peak only. Thus, $\Delta\mu_a$ could be expressed as

$$\begin{aligned} \Delta\mu_a = \Delta c_{\mathrm{mTHPC}}\varepsilon_{\mathrm{mTHPC}} + \Delta c_{\mathrm{Hb}}\varepsilon_{\mathrm{Hb}} + \Delta c_{\mathrm{HbO}}\varepsilon_{\mathrm{HbO}} + AM(\lambda) \\ + \sum_{i=0}^{2}\omega_i C_i \lambda^i, \end{aligned} \quad (6)$$

where the Δc's denote concentration changes; the ε's are the corresponding extinction coefficients; and $M(\lambda)$ and A are the sensitizer fluorescence spectrum and fluorescence amplitude, respectively. The last summation on the right-hand side of Eq. (6) was included to account for tissue autofluorescence overlapping the absorption signals. The number of components within this summation was determined empirically by minimizing the residuals returned by the algorithm. The magnitude of $M(\lambda)$ and the weights ω_i were chosen to match the magnitudes of the chromophore extinction coefficients. For each absorption spectrum, the SVD algorithm returned the chromophore concentrations, i.e., the Δc's, the mTHPC fluorescence amplitude A, and the individual C_i's. The $\Delta c_{\mathrm{mTHPC}}$ was used to predict the mTHPC concentration from each measurement. The sensitizer level was determined by the average $\Delta c_{\mathrm{mTHPC}}$ from two to five absorption spectra acquired for each animal, tissue type, and investigation time point, i.e., at 0 and 4 or 6 h. For the absorption spectroscopy data, the error of the fit was quantified as

$$r = \left[\frac{1}{m-1}\sum_{\lambda}(y_{\mathrm{measured},\lambda} - y_{\mathrm{fit},\lambda})^2\right]^{1/2}, \quad (7)$$

where the summation includes the spectral fitting interval 500 to 800 nm, and m denotes the number of data points within this interval. In the case of negative sensitizer concentration prediction, the mTHPC concentration was set to zero and the error of the fit was reevaluated by only including deoxy- and oxyhemoglobin in the SVD algorithm.

Figure 1(a) illustrates the different basis spectra used for the SVD algorithm within the spectral fitting range. Figure 1(b) shows *in vivo* data from a lesion 4 h after sensitizer administration together with the fit and the corresponding residuals. For this measurement, the predicted concentrations were 1.3, 11.6, and 8.9 μM for mTHPC, deoxy-, and oxyhemoglobin. The mTHPC fluorescence amplitude was $+1.7 \times 10^{-6}$ a.u. (arbitrary units). Note that the analysis of the absorption spectra assumes homogeneous medium. For this situation, the accuracy of the setup and method of data analysis was confirmed in TiO-based liquid phantoms with scattering similar to those levels encountered in normal tissue ($\mu_s' \sim 5$ to 15 cm^{-1}) and sensitizer concentration between 2 and 20 μM. The lower mTHPC detection limit was approximately 0.5 μM within the same set of liquid phantoms as described in Sec. 2.3.

2.5 *Extraction*

Tissue samples, weighing 100 to 200 mg, were homogenized in 3 ml of dimethyl sulfoxide (DMSO) at 24,000 rpm (T18 Basic Ultra Turrax, IKA, Staufen, Germany). The homogenate was centrifuged at 800 g (3000 rpm) for 20 min (EconoSpin, Sorvall Instruments DuPont, Wilmington, Delaware). The su-

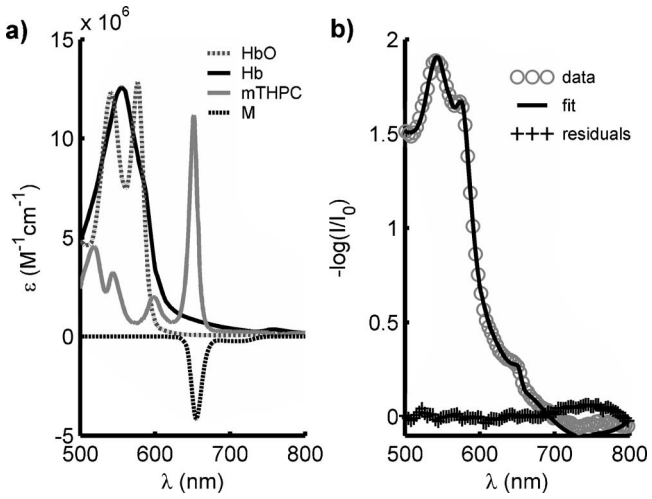

Fig. 1 (a) mTHPC fluorescence and extinction coefficients of mTHPC in ethanol, deoxy- (Hb) and oxyhemoglobin (HbO). The components constituting the background signal are not shown for purpose of clarity. Absorption and fluorescence data for mTHPC was kindly provided by biolitec AG. (b) Absorption data from animal 2. Also shown are the fit and the corresponding residuals. The error of the fit was 0.029.

pernatant was collected and following excitation at 420 nm, the fluorescence signal was recorded between 460 and 700 nm using a luminescence spectrometer (LS 45, Perkin Elmer, Buckinghamshire, UK). The detected fluorescence intensity at 652 nm was used to provide an absolute measure of sensitizer concentration after appropriate calibration. Blood samples were centrifuged at 360 g (2000 rpm) for 10 min to separate out the plasma. Fifty microliters of plasma were mixed with 2950 μl DMSO for further analysis according to the same procedure as for the other organs. The lower detection limit for the extraction setup was 0.04 ng mTHPC/mg tissue, which corresponds to approximately 0.06 μM assuming a tissue density of 1.06 g/ml.

2.6 *Statistical Analysis*

To study agreement between two methods, the correlation of the data from each technique was calculated using:

$$R(x,y) = \frac{\mathrm{cov}(x,y)}{[\mathrm{cov}(x,x)\mathrm{cov}(y,y)]^{1/2}}. \quad (8)$$

Here, $\mathrm{cov}(x,y) = E[(x-m_x)(y-m_y)]$, where E denotes the mathematical expectation, x and y represent the mTHPC quantity as determined by each method, and m_x and m_y are the corresponding averaged mTHPC quantities. For comparison of two means, a two-sided Student's t test was used, where $P \leqslant 0.05$ was considered significant.

3 Results

The extraction results indicated preferential accumulation of mTHPC in lesions as compared to normal skin both at 4 and 6 h after sensitizer application. The average mTHPC concentration in lesions was 6.0 ng/mg tissue with a SD of 3.1 ng/mg. No significant difference could be identified between the two drug-light intervals. Sensitizer levels in liver, spleen, blood, muscle, and normal skin where no mTHPC-gel had been applied were below the detection limit, indicating mTHPC concentrations below 0.04 ng/mg tissue.

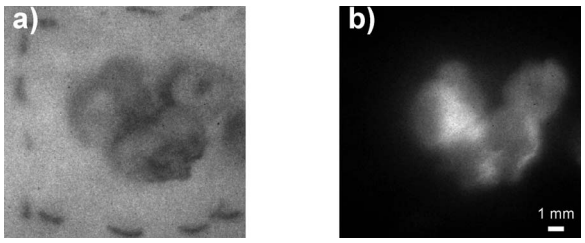

Fig. 2 (a) Room-light image showing lesions and surrounding skin for animal 3 and (b) fluorescence signal at 654 nm showing selective accumulation of mTHPC.

Figure 2 shows room-light and 654-nm fluorescence images of three lesions 4 h after application of the mTHPC-containing gel. The temporal profile of the mTHPC buildup assessed by the fluorescence imaging technique is shown in Fig. 3(a), where the averaged contrast function value is plotted as a function of mTHPC-gel application time for lesion (t), normal skin (n), and skin surrounding the visible lesion (tn). The data indicated significant sensitizer selectivity within lesions for the 4- but not the 6-h drug-light interval. Only normal skin (n) indicated a significant difference between 4- and 6-h application times.

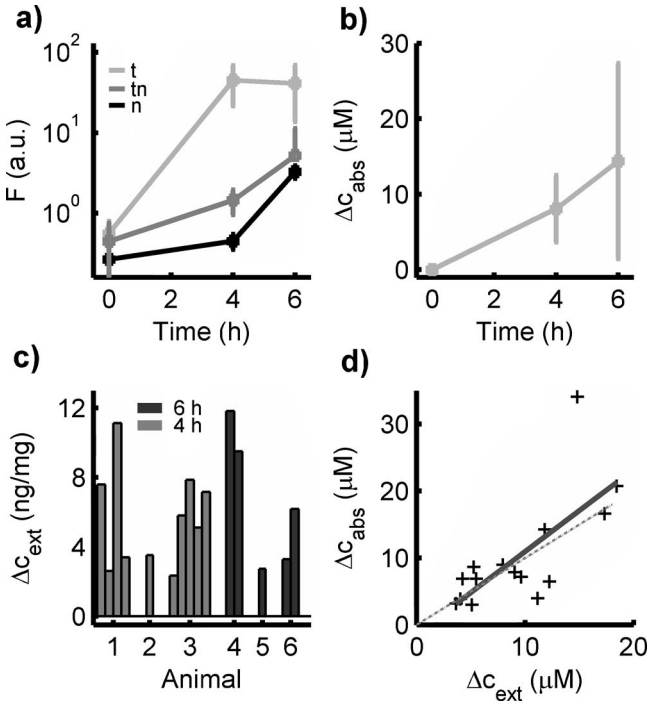

Fig. 3 (a) Contrast function value for normal tissue (n), tissue in close proximity to lesion (tn), and lesion (t). Each marker represents the averaged F value and error bars denote ±1 SD. (b) Temporal profile of the average mTHPC concentration within lesions as estimated by the absorption spectroscopy probe. (c) mTHPC concentration as determined by extraction for each lesion in six animals. (d) Scatter plot illustrating the covariance between absorption and extraction data for all lesions.

As for the extraction data but in contrast to the fluorescence results, the absorption spectroscopy data revealed a selective sensitizer accumulation within lesions for both drug-light intervals. The temporal profile of the calculated mTHPC concentration within lesions is shown in Fig. 3(b). For this tissue type, no significant differences in sensitizer buildup could be identified for the two different mTHPC accumulation times. Resulting mTHPC levels for normal skin and intact skin in close proximity to the lesion were below the detection limit of the setup and are therefore not shown. The model for the SVD algorithm, including mTHPC, deoxy- and oxyhemoglobin extinction coefficients, and mTHPC fluorescence, resulted in good agreement with measurement data. The average fitting errors, evaluated according to Eq. (7), were 0.064 and 0.050 for lesion and intact skin in close proximity to the lesion, respectively. The fitting errors displayed no statistically significant differences with tissue type and drug-light interval.

Figure 3(c) shows the extraction data for each individual lesion, illustrating large intertumor variations in sensitizer concentration. In general, lesions displayed a heterogeneous tissue structure sometimes also presenting necrotic areas. The high variability in mTHPC concentration was most likely influenced by the differences in tissue composition. Figure 3(d) is a scatter plot illustrating the agreement between absorption and extraction data where each marker represents data from a specific lesion. The solid line shows the best fit in a linear least-squares sense, whereas the dashed line represents the ideal fit. The slope of the correlation curve was 1.2. The overestimation of the mTHPC concentration by the absorption data is mostly due to the outlier at $>30\ \mu$M as measured by the absorption technique. For tumor tissue, the absorption and extraction data showed a significant correlation ($P<0.05$) with a correlation coefficient of 0.72. On the other hand, the fluorescence contrast ratio displayed no significant correlation to the other methods.

Figure 4(a) is a photograph of one excised lesion, approximately 4 mm in depth, sliced parallel to its depth axis. The fluorescence contrast function image of the same lesion is presented in Fig. 4(b), illustrating the heterogeneous structure of the mTHPC content. Figure 4(c) shows the fluorescence contrast value (F value) along the depth profile marked by the thin dashed line in Fig. 4(b). As a comparison, the average (±1 SD) F value for all lesions *in vivo* is also included in the graph. The mTHPC concentration assessed by the absorption technique is plotted in Fig. 4(d) for three measurement positions, also showing the decrease in sensitizer concentration with depth. Possibly due to the administration of a total of three 20-μl aliquots of the mTHPC-gel, *in vivo* absorption measurements on this lesion via the surface of the intact tumor indicated sensitizer levels slightly higher than for the remaining animals as tested by a one-sided Student's t test ($P\leqslant 0.05$). The second lesion used for investigating the sensitizer depth penetration did not display significantly higher mTHPC concentration as compared to the other lesions. However, some caution should be exercised when interpreting the sensitizer depth distribution from Fig. 4.

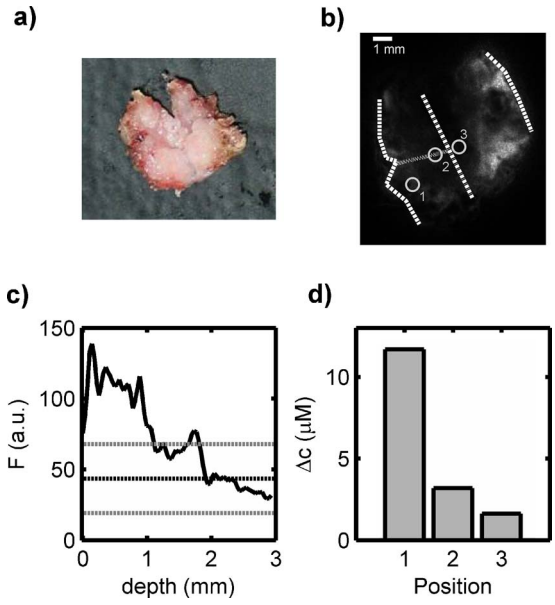

Fig. 4 (a) Digital photograph showing cross section of a vertical cut through a tumor. (b) Fluorescence contrast function image for the same tumor. The tumor surface and deepest tissue region are indicated by the bright dashed lines. (c) Fluorescence contrast function value along the thin dashed line in (b). The dashed lines indicate the average F value ±1 SD for all lesions. (d) mTHPC concentration as measured by the absorption spectroscopy probe. Measurement positions are marked in (b).

4 Discussion

Topical application of ALA was successfully used in combination with superficial PDT of skin malignancies.[7] By employing methyl esterified ALA-Me, an improved tumor selectivity[8] as well as homogeneous protoporphyrin distribution down to 2 mm in human BCCs (Ref. 9) was achieved. However, protoporphyrin IX remains a PDT agent resulting in relatively limited treatment efficacies.[7,13]

This paper reports on the first use of a topically applied liposomal mTHPC-formulation in a nonmelanoma skin carcinoma model. This mTHPC-gel was investigated as a possible alternative to ALA-PDT and systemic administration of mTHPC, suffering from poor treatment outcome for thicker lesions and prolonged photosensitivity, respectively. In this study, significant sensitizer selectivity in lesions as compared to skin with intact stratum corneum was observed from extraction and optical absorption data for both 4- and 6-h drug-light intervals. In fact, the mTHPC concentration within tissue characterized by an undamaged upper skin layer was below the detection limits of these setups. The extraction results from internal organs and normal skin where no mTHPC-gel had been applied showed no trace of the sensitizer, indicating undetectable levels of generalized photosensitivity. Data from the fluorescence imaging setup also indicated no significant variation in sensitizer concentration within lesions for the two application times. However, increased mTHPC fluorescence was observed between the 4- and 6-h application times for gel-treated normal skin with an intact stratum corneum, possibly due to the higher sensitivity of this setup. For the fluorescence spectroscopy data set, the selectivity between lesion and normal skin was thus only significant for the shorter drug-light interval, indicating an optimal drug-light interval of 4 h for the present skin tumor model.

The observed sensitizer distribution is likely due to differences in the ability of mTHPC and liposomes to penetrate the tissue layers. The absence of stratum corneum over the lesion seems to facilitate the sensitizer penetration, whereas intact skin prevents the lower tissue layers from accumulating any substantial amount of mTHPC. Supporting the present observations, Schmid and Karting state that intact liposomes penetrate only very superficial parts of the normal epidermis, whereas damaged skin constitutes a less efficient barrier.[32] The diffusion of liposome-encapsulated ALA through healthy mouse skin has been shown to require tens of hours,[20] and this slow process could be explained by the way liposomes are believed to interact with intact skin, first adhering to and then disrupting the upper tissue membranes. The liposomes hence act as penetration enhancers.[19] These previously published results are in agreement with the increasing, although still low, mTHPC levels found in normal mouse skin for the 6-h administration time.

For tumor tissue, the large variations in mTHPC concentration and the lack of significant differences between 4- and 6-h drug-light intervals could be due to a sensitizer buildup within lesions mostly determined by the tissue composition and the status of the uppermost layers. For example, it was noted that necrotic regions displayed overall lower sensitizer levels. It is also reasonable to suspect the depth penetration of the sensitizer to depend on the status of the upper skin layers. Within the lesions for which the sensitizer depth penetration was investigated, the mTHPC concentration was in the micromolar range to depths of 3 to 4 mm. Similar results were reported by Peng et al.,[9] where good selectivity and homogeneous sensitizer distribution down to 2 mm in human BCCs were observed following topical application of ALA-Me. Since the liposomal mTHPC formulation was not compared to its pure analog, it is difficult to determine the effect the use of liposomes had on the sensitizer distribution and depth penetration within this study.

The mTHPC levels observed within lesions in this study are in the range shown to induce significant PDT effects once irradiated at an appropriate wavelength.[33] However, another factor important to the PDT outcome is the localization of the sensitizer molecule within the tissue and the cell. In the case of systemic mTHPC administration, short drug-light intervals result[33] in vascularly targeted PDT, whereas longer time periods enable the sensitizer to localize within the cells, targeting, for example, mitochondria.[34] In the case of topical mTHPC administration, the mTHPC levels found in blood were low for all time points investigated. We thus anticipate the PDT effect to more strongly correlate with maximum sensitizer concentration within the lesion and display less pronounced vascular effects.

In parallel with the extraction study, fluorescence imaging and absorption spectroscopy were evaluated as noninvasive methods for assessing sensitizer content *in vivo*. The fluorescence imaging setup has the advantage of being a more sensitive tool than the absorption spectroscopy probe. Furthermore, the ability to image larger areas quickly provides valuable information on the spatial sensitizer distribution. However, for the range of optical properties found in biological tissue, the effective penetration depth of the near-UV light used for exciting the mTHPC fluorescence is of the order of a couple of hundred micrometers, making the fluorescence imaging method applicable only when studying very superficial tissue regions. In addition, the fluorescence signal is highly dependent on tissue optical properties, making it difficult to use the absolute fluorescence level as a reliable concentration estimate. Within this study, the surface of the lesions displayed a heterogeneous structure, sometimes including superficial areas of dark necrotic regions. The shallow investigation volume in combination with sensitivity to the optically heterogeneous tissue could thus explain the lack of significant correlation between extraction and fluorescence data.

In contrast to the fluorescence signal, the absorption spectroscopy data correlated rather well with the extraction results. One reason for the better agreement could be the higher overlap of probing volume of the two methods. A previous publication has reported on approximate probing depth of 1 to 2 mm for the absorption probe,[28] matching the depth of skin tumors likely to be treated by PDT using topical irradiation. In addition, since the analysis of the absorption spectrum takes into account the average tissue chromophore content, these results are not as easily corrupted by variations in tissue optical properties as is the fluorescence data. However, the relatively high detection limit for the absorption spectroscopy probe is a major drawback. It is therefore highly desirable to combine the sensitivity of the fluorescence level with the ability of the absorption signal to account for varying tissue absorption. Finlay and Foster demonstrated a probe combining white-light absorption with fluorescence spectroscopy to recover the intrinsic tissue autofluorescence, i.e., the fluorescence spectra corrected for tissue absorption and scattering.[35] By utilizing the absorption spectrum to assess the tissue optical properties, the corrected fluorescence signal would constitute a more reliable fluorophore concentration estimate. A further drawback of the absorption spectroscopy probe is the inherent sensitivity to measurement site within the spatially heterogeneous structure of the lesions. The latter effect most likely explains part of the scattered appearance of the absorption data in relation to the ideal fit in Fig. 3(d). Furthermore, the outlier at $>30\ \mu$M as measured by the absorption spectroscopy setup could possibly be due to a small amount of mTHPC-gel remaining on the skin surface due to its inherent roughness. This effect highlights the importance of careful cleansing of the tissue surface prior to optical measurements in order to detect the true sensitizer distribution, i.e., the amount of mTHPC that has penetrated into the tissue.

In connection with this discussion, note the importance of including the mTHPC fluorescence as one of the components of the SVD algorithm. The shorter wavelengths present in the output from the xenon arc lamp induce sensitizer fluorescence overlapping the absorption peak at 652 nm. In contrast to the effective path length, the fluorescence level is dependent on the sample scattering for this source-detector separation. Although this was not taken into account in the analysis process as it was outlined in Sec. 2.4, including the fluorescence component significantly improved the accuracy of the setup. By simply excluding the sensitizer fluorescence component from the analysis resulted in underestimation of the sensitizer concentration by a factor of 1.5 for the investigated lesions. Furthermore, if also limiting the spectral fitting range to 630 to 750 nm to avoid the strong hemoglobin absorption bands, the mTHPC concentration was underestimated by a factor 2. We conclude that sensitizer fluorescence should be

taken into account when utilizing the tissue absorption imprint for absolute concentration estimates. A significant underestimation has also been reported by Weersink et al. when utilizing a reflectance spectroscopy probe with multiple source-detector fibers for determining $AlPcS_4$ concentration in *in vivo* rabbit skin.[36] The underestimation of the sensitizer concentration by a factor of 3 was attributed the layered skin structure and nonuniform $AlPcS_4$ distribution. Within our work, the investigated tissue was highly heterogeneous also presenting a depth-dependent sensitizer concentration. Therefore, these effects constitute another source of error as they were not considered in our current evaluation of the optical absorption signal, which assumes homogeneous medium.

In conclusion, we reported on the use of a topically administered mTHPC formulation in a murine skin tumor model. In this sensitizer formulation, the hydrophobic mTHPC molecule was incorporated into conventional liposomes, rendering the sensitizer preparation water soluble. By administering the compound via a heat-setting gel, the retention time of the applied gel could be increased. Fluorescence and absorption spectroscopy as well as extraction data indicated significant mTHPC accumulation within lesions but no difference in tumor sensitizer concentration between the 4- and 6-h application times. The more sensitive fluorescence setup indicated optimal tumor selectivity for the 4-h drug-light interval. Furthermore, the topical administration route led to low levels of systemic photosensitization. Based on these results, this sensitizer formulation and administration path would be interesting to pursue for topical mTHPC PDT. Currently, a phase I clinical trial has been initiated to study the feasibility of using the mTHPC-gel for treatment of skin tumors.

Acknowledgments

This work was funded by the European Commission (EC) integrated project BRIGHT IST-511-722-2003 and the National Institutes of Health (NIH) Prime Cooperative Agreement No. 1 U54 CA 104677. The authors gratefully acknowledge Irving Bigio at Boston University for providing instrumentation and technical support for the optical absorption spectroscopy setup.

References

1. T. J. Dougherty, C. J. Gomer, B. W. Henderson, G. Jori, D. Kessel, M. Korbelik, J. Moan, and Q. Peng, "Photodynamic therapy," *J. Natl. Cancer Inst.* **90**(12), 889–905 (1998).
2. R. D. Almeida, B. J. Manadas, A. P. Carvalho, and C. B. Duarte, "Intracellular signaling mechanisms in photodynamic therapy," *Biochim. Biophys. Acta* **1704**(2), 59–86 (2004).
3. M. Triesscheijn, M. Ruevekamp, M. Aalders, P. Baas, and F. A. Stewart, "Outcome of mTHPC mediated photodynamic therapy is primarily determined by the vascular response," *Photochem. Photobiol.* **81**(5), 1161–1167 (2005).
4. F. H. van Duijnhoven, R. I. J. M. Aalbers, J. P. Rovers, O. T. Terpstra, and P. J. K. Kuppen, "Immunological aspects of photodynamic therapy of liver tumors in a rat model for colorectal cancer," *Photochem. Photobiol.* **78**(3), 235–240 (2003).
5. J. S. Dysart, G. Singh, and M. S. Patterson, "Calculation of singlet oxygen dose from photosensitizer fluorescence and photobleaching during mTHPC photodynamic therapy of MLL cells," *Photochem. Photobiol.* **81**(1), 196–205 (2005).
6. C. Hopper, A. Kubler, H. Lewis, I. BingTan, and G. Putnam, "mTHPC-mediated photodynamic therapy for early oral squamous cell carcinoma," *Int. J. Cancer* **111**(1), 138–146 (2004).
7. Q. Peng, T. Warloe, K. Berg, J. Moan, M. Kongshaug, K.-E. Giercksky, and J. M. Nesland, "5-aminolevulinic acid-based photodynamic therapy: Clinical research and future challenges," *Cancer* **79**, 2282–2308 (1997).
8. P. Juzenas, S. Sharfaei, J. Moan, and R. Bissonnette, "Protoporphyrin IX fluorescence kinetics in UV-induced tumours and normal skin of hairless mice after topical application of 5-aminolevulinic acid methyl ester," *J. Photochem. Photobiol., B* **67**(1), 11–17 (2002).
9. Q. Peng, A. M. Soler, T. Warloe, J. M. Nesland, and K. E. Giercksky, "Selective distribution of porphyrins in skin thick basal cell carcinoma after topical application of methyl 5-aminolevulinate," *J. Photochem. Photobiol., B* **62**(3), 140–145 (2001).
10. S. Mitra and T. H. Foster, "Carbogen breathing significantly enhances the penetration of red light in murine tumours *in vivo*," *Phys. Med. Biol.* **49**(10), 1891–1904 (2004).
11. Q. G. Ren, S. M. Wu, Q. Peng, and Y. J. Chen, "Comparison of 5-aminolevulinic acid and its hexylester mediated photodynamic action on human hepatoma cells," *Acta Biochim. Biophys. Sinica* **34**(5), 650–654 (2002).
12. E. Balasubramaniam and P. Natarajan, "Photophysical properties of protoporphyrin IX and thionine covalently attached to macromolecules," *J. Photochem. Photobiol., A* **103**(3), 201–211 (1997).
13. P. Schleier, A. Berndt, S. Kolossa, and M. Wood, "Comparison between mALA- and ALA-PDT in the treatment of basal cell carcinomas," *Oral Oncol. Suppl.* **1**(1), 67–68 (2005).
14. S. Mitra and T. H. Foster, "Photophysical parameters, photosensitizer retention and tissue optical properties completely account for the higher photodynamic efficacy of meso-tetra-hydroxyphenyl-chlorin vs Photofrin," *Photochem. Photobiol.* **81**(4), 849–859 (2005).
15. S. Sasnouski, V. Zorin, I. Khludeyev, M. A. D'Hallewin, F. Guillemin, and L. Bezdetnaya, "Investigation of Foscan interactions with plasma proteins," *Biochim. Biophys. Acta* **1725**(3), 394–402 (2005).
16. P. Westerman, T. Glanzmann, S. Andrejevic, D. R. Braichotte, M. Forrer, G. A. Wagnieres, P. Monnier, H. van den Bergh, J. P. Mach, and S. Folli, "Long circulating half-life and high tumor selectivity of the photosensitizer meta-tetrahydroxyphenylchlorin conjugated to polyethylene glycol in nude mice grafted with a human colon carcinoma," *Int. J. Cancer* **76**(6), 842–850 (1998).
17. J. P. Keene, D. Kessel, E. J. Land, R. W. Redmond, and T. G. Truscott, "Direct detection of singlet oxygen sensitized by haematoporphyrin and related compounds," *Photochem. Photobiol.* **43**(2), 117–120 (1986).
18. G. Gupta, C. A. Morton, C. Whitehurst, J. V. Moore, and R. M. Mackie, "Photodynamic therapy with meso-tetra(hydroxyphenyl) chlorin in the topical treatment of Bowen's disease and basal cell carcinoma," *Br. J. Dermatol.* **141**(2), 385–386 (1999).
19. M. J. Choi and H. I. Maibach, "Liposomes and niosomes as topical drug delivery systems," *Skin Pharmacol. Appl. Skin Physiol.* **18**(5), 209–219 (2005).
20. M. B. Pierre, A. C. Tedesco, J. M. Marchetti, and M. V. Bentley, "Stratum corneum lipids liposomes for the topical delivery of 5-aminolevulinic acid in photodynamic therapy of skin cancer: preparation and *in vitro* permeation study," *BMC Dermatol.* **1**(1), 5 (2001).
21. X. Damoiseau, H. J. Schuitmaker, J. W. M. Lagerberg, and M. Hoebeke, "Increase of the photosensitizing efficiency of the Bacteriochlorin a by liposome-incorporation," *J. Photochem. Photobiol., B* **60**(1), 50–60 (2001).
22. A. M. Richter, "Liposomal delivery of a photosensitizer, benzoporphyrin derivative monoacid ring A (BPD), to tumor tissue in a mouse tumor model," *Photochem. Photobiol.* **57**, 1000–1006 (1993).
23. C. af Klinteberg, A. M. K. Enejder, I. Wang, S. Andersson-Engels, S. Svanberg, and K. Svanberg, "Kinetic fluorescence studies of 5-aminolaevulinic acid-induced protoporphyrin IX accumulation in basal cell carcinomas," *J. Photochem. Photobiol., B* **49**(2–3), 120–128 (1999).
24. J. R. Mourant, I. J. Bigio, D. A. Jack, T. M. Johnson, and H. D. Miller, "Measuring absorption coefficients in small volumes of highly scattering media: source-detector separations for which path lengths do not depend on scattering properties," *Appl. Opt.* **36**(22), 5655–5661 (1997).
25. B. Pegaz, E. Debefve, J. P. Ballini, G. Wagnieres, S. Spaniol, V. Albrecht, D. V. Scheglmann, N. E. Nifantiev, H. van den Bergh, and Y. N. Konan-Kouakou, "Photothrombic activity of m-THPC-loaded liposomal formulations: pre-clinical assessment on chick chorioallantoic membrane model," *Eur. J. Pharm. Sci.* **28**, 134–140 (2006).
26. M. Kyriazi, D. Yova, M. Rallis, and A. Lima, "Cancer chemopreven-

tive effects of Pinus Maritima bark extract on ultraviolet radiation and ultraviolet radiation-7,12,dimethylbenz(a)anthracene induced skin carcinogenesis of hairless mice," *Cancer Lett.* **237**(2), 234–241 (2006).
27. C. H. Gallagher, P. J. Canfield, G. E. Greenoak, and V. E. Reeve, "Characterization and histogenesis of tumors in the hairless mouse produced by low-dosage incremental ultraviolet radiation," *J. Invest. Dermatol.* **83**(3), 169–174 (1984).
28. J. R. Mourant, T. M. Johnson, G. Los, and I. J. Bigio, "Non-invasive measurement of chemotherapy drug concentrations in tissue: preliminary demonstrations of in vivo measurements," *Phys. Med. Biol.* **44**(5), 1397–1417 (1999).
29. W. J. Cottrell, A. R. Oseroff, and T. H. Foster, "Portable instrument that integrates irradiation with fluorescence and reflectance spectroscopies during clinical photodynamic therapy of cutaneous disease," *Rev. Sci. Instrum.* **77**(6), 064302 (2006).
30. E. L. Hull, M. G. Nichols, and T. H. Foster, "Quantitative broadband near-infrared spectroscopy of tissue-simulating phantoms containing erythrocytes," *Phys. Med. Biol.* **43**(11), 3381–3404 (1998).
31. S. A. Prahl, "Tabulated molar extinction coefficient for hemoglobin in water," http://omlc.ogi.edu/spectra/hemoglobin/summary.html (1999).
32. M. H. Schmid and H. C. Korting, "Therapeutic progress with topical liposome drugs for skin disease," *Adv. Drug Delivery Rev.* **18**(3), 335–342 (1996).
33. P. Cramers, M. Ruevekamp, H. Oppelaar, O. Dalesio, P. Baas, and F. A. Stewart, "Foscan® uptake and tissue distribution in relation to photodynamic efficacy," *Br. J. Cancer* **88**(2), 283–290 (2003).
34. C. M. N. Yow, J. Y. Chen, N. K. Mak, N. H. Cheung, and A. W. N. Leung, "Cellular uptake, subcellular localization and photodamaging effect of Temoporfin (mTHPC) in nasopharyngeal carcinoma cells: comparison with hematoporphyrin derivative," *Cancer Lett.* **157**(2), 123–131 (2000).
35. J. C. Finlay and T. H. Foster, "Recovery of hemoglobin oxygen saturation and intrinsic fluorescence with a forward-adjoint model," *Appl. Opt.* **44**(10), 1917–1933 (2005).
36. R. A. Weersink, J. E. Hayward, K. R. Diamond, and M. S. Patterson, "Accuracy of noninvasive *in vivo* measurements of photosensitizer uptake based on a diffusion model of reflectance spectroscopy," *Photochem. Photobiol.* **66**(3), 326–335 (1997).